Monitoring and trend mapping of sea surface temperature (SST) from MODIS data: a case study of Mumbai coast

Samee Azmi · Yogesh Agarwadkar ·
Mohor Bhattacharya · Mugdha Apte ·
Arun B. Inamdar

Abstract Sea surface temperature (SST) is one of the most important parameters in monitoring ecosystem health in the marine and coastal environment. Coastal ecosystem is largely dependent on ambient temperature and temperature fronts for marine/coastal habitat and its sustainability. Hence, thermal pollution is seen as a severe threat for ecological health of coastal waters across the world. Mumbai is one of the largest metropolises of the world and faces severe domestic and industrial effluent disposal problem, of which thermal pollution is a major issue with policy-makers and environmental stakeholders. This study attempts to understand the long-term SST variation in the coastal waters off Mumbai, on the western coast of India, and to identify thermal pollution zones. Analysis of SST trends in the near-coastal waters for the pre- and post-monsoon seasons from the year 2004 to the year 2010 has been carried out using Moderate Resolution Imaging Spectro-radiometer (MODIS) Thermal Infra-red (TIR) bands. SST is calculated with the help of bands 31 and 32 using split window method. Several statistical operations were then applied to find the seasonal averages in SST and the standard deviation of SST in the study area. Maximum variation in SST was found within a perpendicular distance of 5 km from the shoreline during the study period. Also, a warm water mass was found to form consistently off coast during the winter months. Several anthropogenic sources of thermal pollution could be identified which were found to impact various locations along the coast.

Keywords Sea surface temperature · Remote sensing · Spatio-temporal trends · Marine and coastal environment · MODIS

Introduction

Coastal waters are part of the marine environment as well as the boundary of terrestrial ecosystems. These ecotones are as fragile as they are rich in minerals, crude oil, fish resource, etc. They are also used for disposal of wastes from coastal cities. Thermal pollution of rivers and coastal seas by heated efflux released from industrial sources is a serious environmental problem which causes destruction and imbalance of aquatic life. Many aquatic life-forms are temperature sensitive.

The temperature rise in water body due to thermal effluents can have a cascading effect on the aquatic life. Increased temperatures can directly cause mortalities in the fish species. It may also lead to elimination of certain algal species and introduction of undesirable species. High temperatures can adversely affect the metabolic rates, growth and reproduction. It could also lead to depletion of certain species.

Increase in water temperature also causes reduction of dissolved oxygen content of the water. This rise in temperature also leads to increased metabolic rates for the fish and greater use of oxygen, and increases

S. Azmi (✉) · Y. Agarwadkar · M. Bhattacharya · M. Apte · A. B. Inamdar
Coastal & Marine Research Laboratory, Centre of Studies in Resource Engineering, IIT Bombay, Mumbai 400076, India
e-mail: samiazmi@gmail.com

photosynthesis, where oxygen is produced (John 1971; Vaquer-Sunyer and Duarte 2011). The balance depends on the supply of nutrient in water. With ample supply of nutrients and increased water temperature, the green and blue-green algae become more active, leading to accelerated eutrophication. (John 1971)

Physicochemical constituents of water body may be disturbed due to thermal discharge which might affect the species composition. Increase in vegetation period and cell size may be observed in phytoplanktons and other marine macrophytes which might result in increased productivity depending on the available nutrient in water. Change in temperature also affects the benthic fauna. (Kulkarni et al. 2011)

The coastal marine environment beside Mumbai, India, constitutes a variety of flora and fauna (Verma et al. 2004) including a rich mangrove growth along Thane, Malad, Manori and Mahul creeks. According to the classification proposed by Central Pollution Control Board (Government of India), the central west coast of India including northern Karnataka, Goa and southern Maharashtra is grouped under the class SW-1, which is supposed to include salt pans, mariculture, contact water sports and ecologically sensitive areas (Varkey 1999). The main sources of pollution of the Mumbai coast are urban sewage, runoff, nutrient pollution and thermal discharges (Gupta et al. 2006).

Availability of satellite data has enabled observation of atmospheric states and processes at various scales varying spatially and/or temporally. Since 1970, remotely sensed imagery has been used to map and monitor coastal areas (Yang et al. 2013). Various aspects such as water quality, coastal dynamics, terrestrial and marine habitats and certain coastal hazards are being monitored using satellite images (McClain 2009). The use of this method has
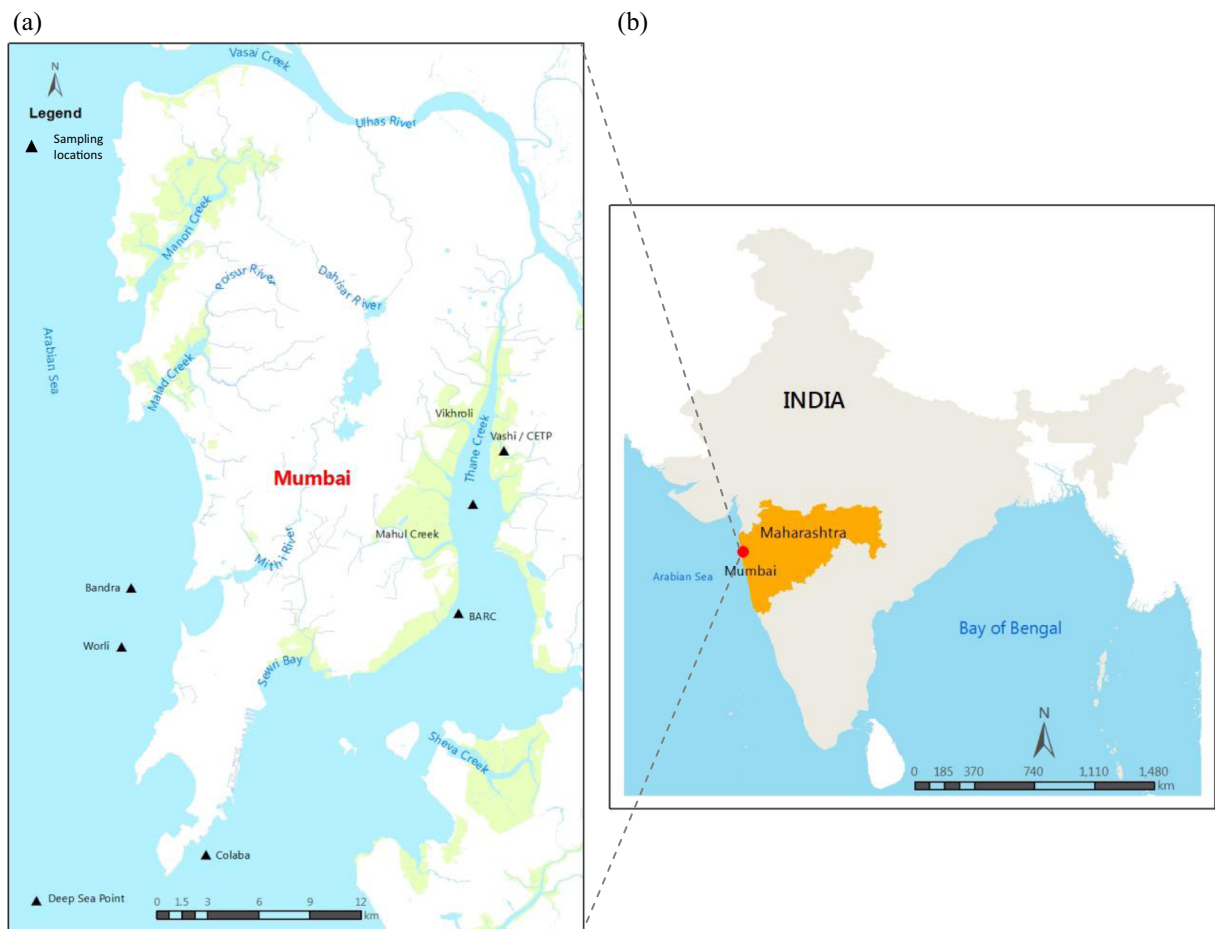
(a)   (b)

Fig. 1 a Study area map with water sampling locations. b Location map of Maharashtra, India
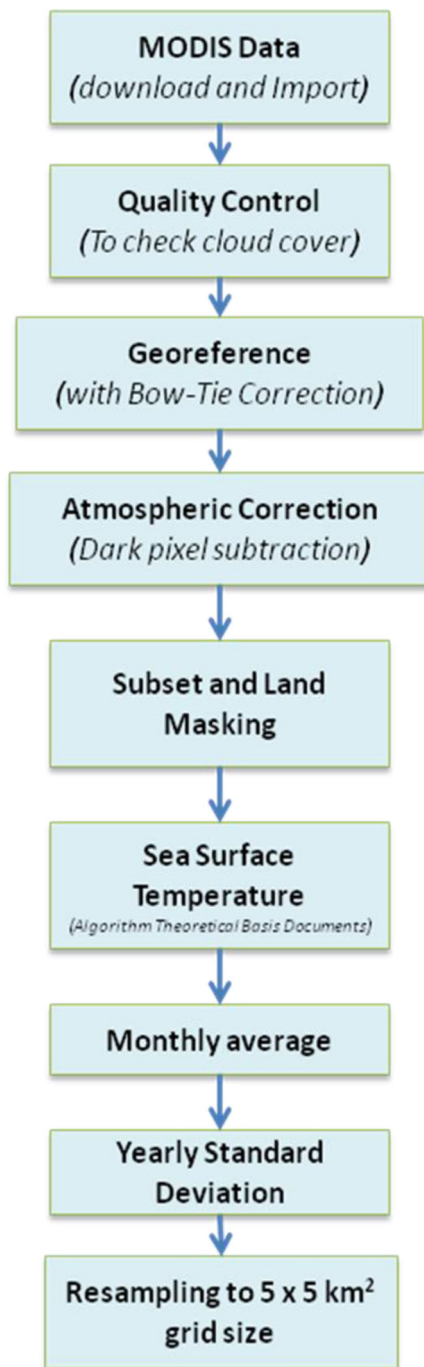
MODIS Data
(download and Import)

Quality Control
(To check cloud cover)

Georeference
(with Bow-Tie Correction)

Atmospheric Correction
(Dark pixel subtraction)

Subset and Land Masking

Sea Surface Temperature
(Algorithm Theoretical Basis Documents)

Monthly average

Yearly Standard Deviation

Resampling to 5 x 5 km² grid size

Fig. 2 Flowchart of the methodology followed

gained importance in understanding the behaviour of coastal environments because of its capacity to provide spatio-temporal information cost-effectively. Moreover, the importance of time series imagery and derived products, for showing space-time cube dynamics in coastal and marine environment on longer time scales, is widely recognized, especially in relation to climatic variability. The present study proposes to map and monitor the thermal pollution of coastal waters off Mumbai, India, using remote sensing and GIS techniques.

Study area

The study area, as shown in Fig. 1, comprises the coastal and offshore waters of Mumbai, falling within the latitude-longitude coordinates of 19° 8′ 23″ N, 72° 39′ 54″ E and 18° 48′ 26″ N, 72° 58′ 17″ E. The climate of the study area is characterized by summer season from March to June with high atmospheric humidity and heavy southwestern monsoon rainfall. The cold season is mildly cold, occurring between December and February. The period from June to the end of September constitutes the southwest monsoon season. During October and November, the post-monsoon season, the hot and humid spell continues. The month of March sees a mean minimum temperature of 21.1 °C and mean maximum temperature of 33 °C (Meoweather 2013). January is generally the coldest month with the mean daily maximum and minimum temperature at 24 and 18 °C respectively (Gupta 2005).

Approximately 2200 industrial units of various categories engaged in manufacturing of different products discharge 26 MLD of effluent in the sea. Products such as chemicals, dyes, dye intermediates, bulk drugs, pharmaceuticals, textile auxiliaries, pesticides, petrochemicals, textile processors and engineering units are being manufactured. Treated industrial effluent is discharged into Common Effluent Treatment Plant (CETP) for further treatment and later discharged into Thane and Vashi creek (refer to Fig. 1) (MPCB 2010).

Methodology

Analysis done using satellite data provides two main advantages, viz. a comprehensive view of the ocean with frequent revisit images, allowing the synoptic examination of basin-wide ocean surface dynamics that is not possible with ships or buoys. This study aims to analyse the satellite data using the standard procedure of atmospheric correction, pre-processing of the satellite

Table 1 Coefficients for the MODIS_SST retrieval algorithm derived using ECMWF assimilation model (Minnett 1990)

Coefficients		
	$T_{30}-T_{31}\leq0.7$	$T_{30}-T_{31}>0.7$
c_1	1.11071	1.196099
c_2	0.9586865	0.9888366
c_3	0.1741229	0.1300626
c_4	1.876752	1.627125

data and resultant retrieval of sea surface temperature (SST).

Satellite data collection

The Moderate Resolution Imaging Spectro-radiometer (MODIS) is the National Aeronautic and Space Administration's (NASA) 36-band ocean colour sensor onboard the satellites Terra and Aqua. MODIS mission has been providing global SST data since 2000. However, these global SST products come at a binned (averaged) 4-km resolution with coastal mixed pixels, which are then supplied to the user after applying a land mask, which almost fully covers the coastal pixels. Hence, MODIS SST data product (MOD 28) derived from MODIS is rendered unsuitable for study of near-coastal SST plumes and fronts (Masuoka et al. 2000).

Therefore, to satisfy the need of this study, MODIS Thermal Infra-red (TIR) data (bands 31 and 32) with 1-km resolution is used for SST trend generation (year 2004 to 2010), for pre- and post-monsoon season. A basic atmospheric correction by the dark pixel subtraction process has been applied to the satellite data after correction of positional errors such as bow-tie effect. Spectral emissive radiance values were calculated from these pre-processed datasets. An appropriate land mask was applied to the images before calculation of SST to minimize averaging errors between land and sea surface temperature. The flowchart of the procedure followed is given in Fig. 2.

The study is limited by the lack of cloud-free data for the study area. Data was selected on the basis of clear sky, low cloud cover (<5 %) and location of the study area near or on the scene centre (to reduce positional distortions). Data during the monsoons has not been used due to the cloud cover. Almost 60–100 % cloud cover is found during the May–October, making the MODIS data useless for this time of the year. Even the in situ
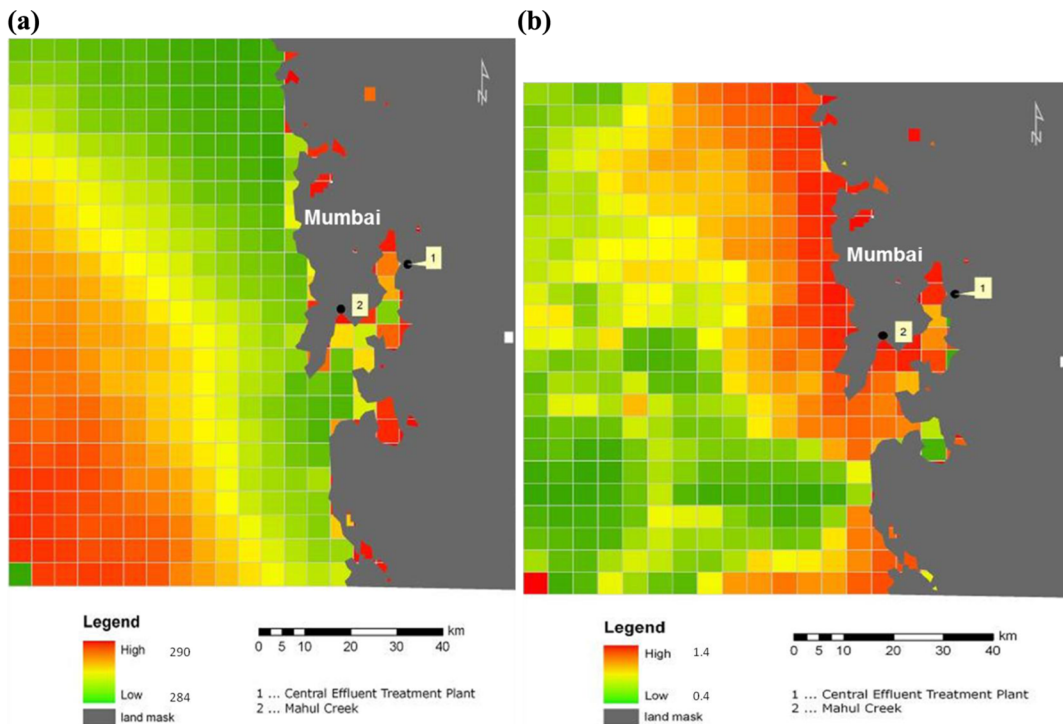

Fig. 3 **a** Monthly aggregated average and **b** standard deviation of SST for December (2004–2009)
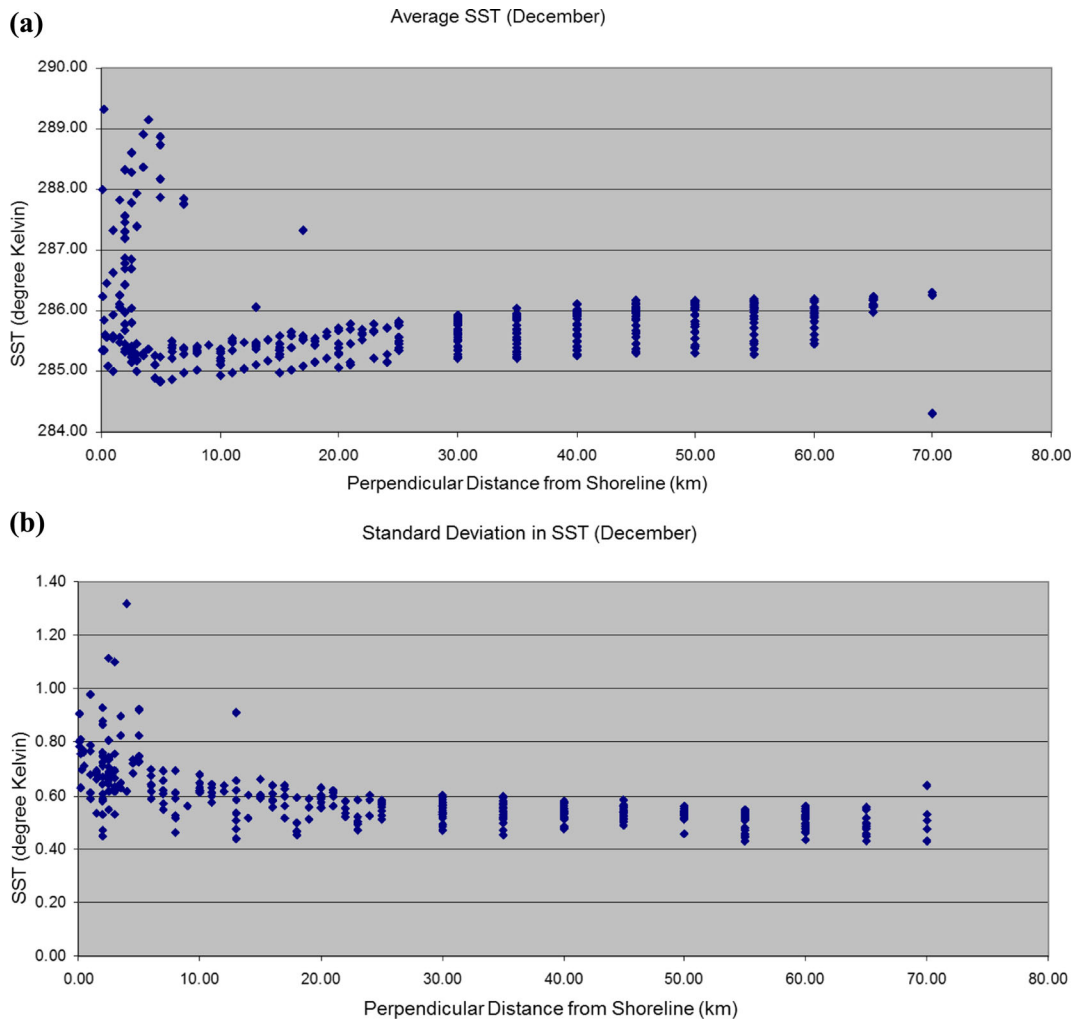
(a)

(b)

Fig. 4 Relationship of **a** average and **b** standard deviation of SST with perpendicular distance from shoreline for December

measurements are not allowed as the sea is rough and unsuitable for venturing in the open sea using small boats.

Estimation of sea surface temperature

For the calculation of SST, first, the brightness temperature was calculated from the spectral emissive radiance data using the following standard formula for Newton-Boltzmann as given in Eq. 1:

$$L = 2*h*c^2*\lambda - 5 / \left[e^{(h*c/k*\lambda*T)} - 1 \right] \qquad (1)$$

where

L is the radiance (watts/m^2/ steradian/m)

h is the Planck's constant (joule-second)
c is the speed of light in vacuum (m/s)
k is the Boltzmann gas constant (joules/kelvin)
λ is the band or detector centre wavelength (m)
T is the temperature (kelvin)

Sea surface temperature was calculated from this brightness temperature data. This temperature is the sea surface skin temperature ranging from 5- to 10-μm depth (Brown et al. 1999). The algorithm implemented for SST calculation is MODIS-SST European Centre for Medium-Range Weather Forecasts (ECMWF) based model, which has been preferred to the radiosonde-based model with similar structure but different coefficients.

According to Minnett (1990), the predicted RMS uncertainty in the SST retrievals using this model is
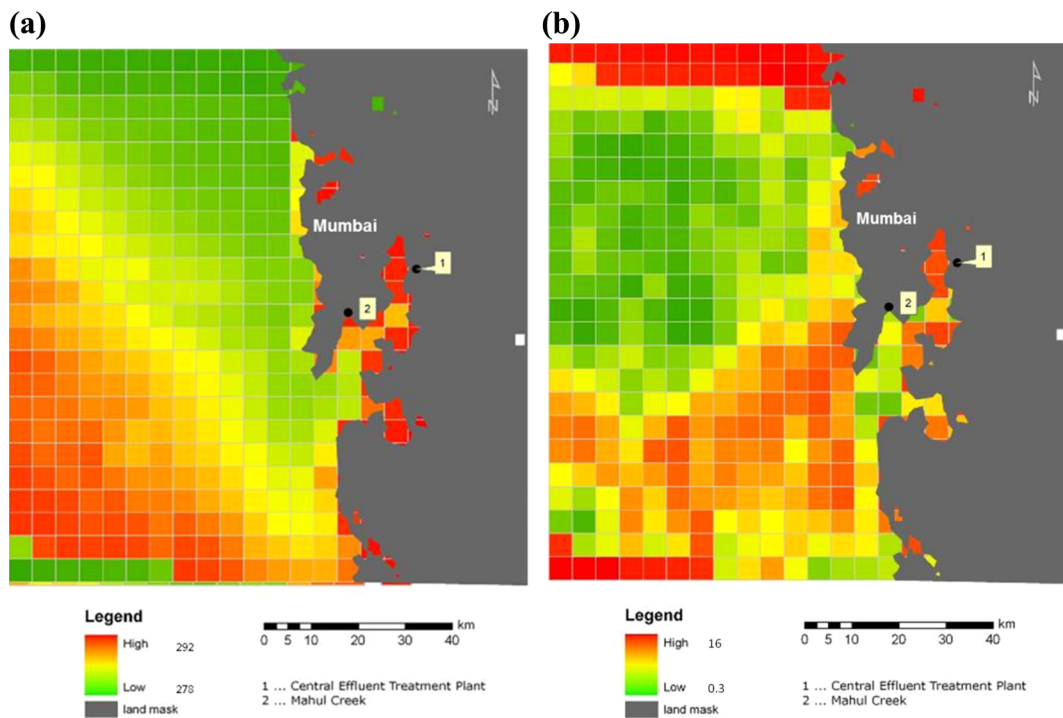
(a)

(b)

Fig. 5 **a** Monthly aggregated average and **b** standard deviation of SST for January (2005–2010)

0.345 K, which is marginally larger than the value for the coefficients derived from the radiosonde model, a result of a wider range of atmospheric conditions represented in this model. These results are based on the output of the ECMWF assimilation model, observed through 'pseudo-sondes' uniformly distributed at 10° latitude and longitude intervals. This model thus carries the advantage of uniformly representing the global range of marine atmospheric condition (Brown et al. 1999).

The algorithm is as given below (Brown et al. 1999):

$$MODIS\_SST = c_1 + c_2*T_{31} + c_3*T_{3132}$$
$$+ c_4*(\sec(\theta)-1)*T_{3132} \quad (2)$$

where

T_{31} is the band 31 brightness temperature (BT)
T_{3132} is (band 32 − band 31) BT difference
θ is the satellite zenith angle

This algorithm differentiates atmospheric vapour load using the difference between the brightness temperatures (T_{3132}) for the 11- and 12-μm bands (MODIS band numbers 31 and 32). Coefficients are determined for T_{3132} greater or less than 0.7 K. While implementing, the coefficients are weighted by the measured T_{3132}.

Coefficients for the MODIS_SST retrieval algorithm derived using ECMWF assimilation model is mentioned in Table 1.

Monthly average SST was generated for every year from 2004 to 2009 for the month of December and 2005–2010 for the months of January and March. These three months have been analysed as they show the maximum variation in SST in largely cloud-free condition. December is the beginning of winter after monsoon season; January is the coldest month of the study area, and March is the transition period from winter to summer. These months show major SST variation and reflect possible anthropogenic sources of increased heat in the waters. Monthly averages then were clumped together for every year (December, January and March averages for the years given above). Standard deviation was calculated for daily images. To generate the SST trends, the 1-km pixel-size images were resampled to a 5 km×5 km grid size. While binning the coastal pixels, land mass was avoided and standard deviation was calculated for water area available and not the entire 5 km×5 km.

The 5-km buffer from land that has been taken in this study as reference to estimate the thermal anomaly in the nearshore waters has been derived from the overall
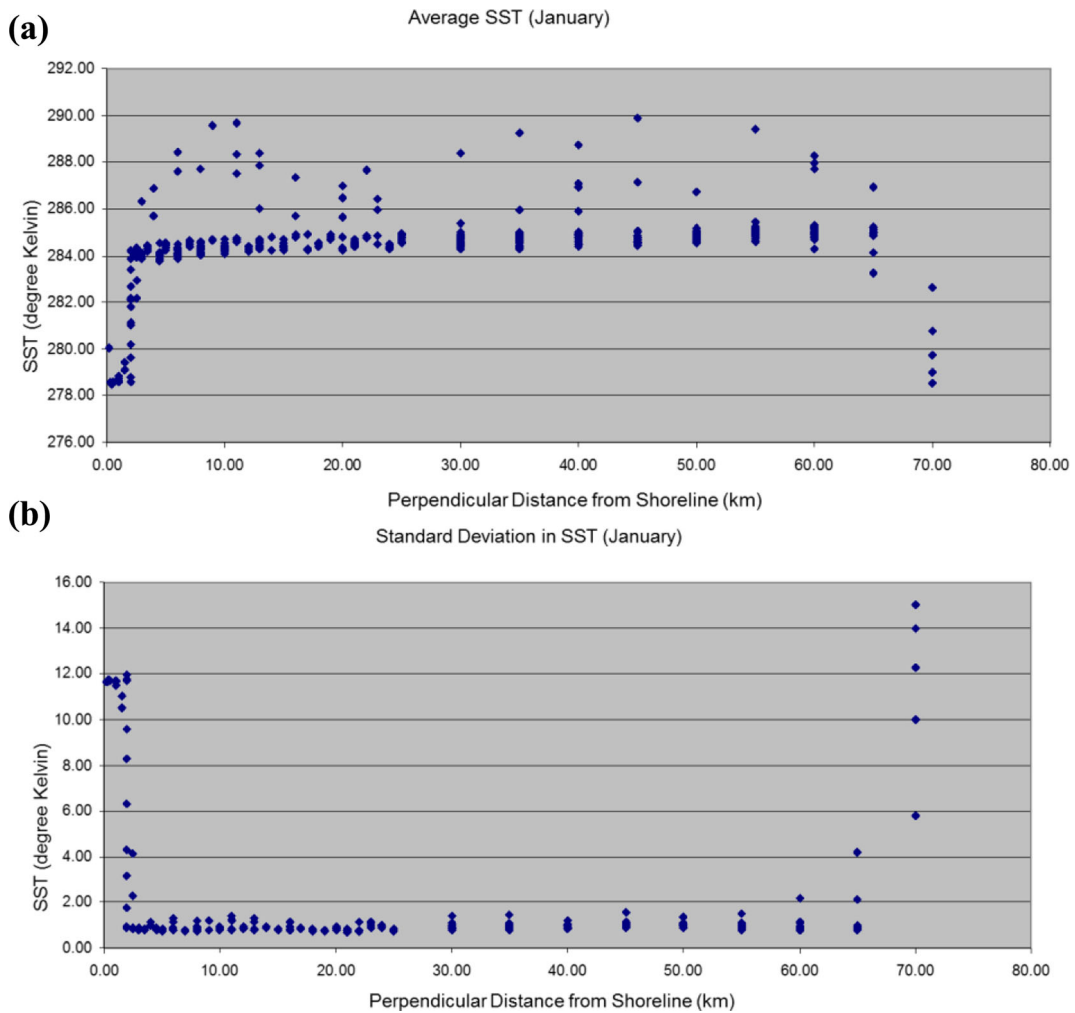
Fig. 6 Relationship of **a** average and **b** standard deviation of SST with perpendicular distance from shoreline for January

standard deviation pattern of SST in the study area. After the 5-km stretch, the waters are found to be quite stable in terms of monthly/ seasonal variability.

Results and discussions

The flora, fauna and microorganisms are affected due to the rise in ambient water temperature. Current work focusses on mapping the trend of SST change. The effect of this temperature change on the various species of organisms is out of scope of the current work due to various factors, mainly data unavailability. This effect of temperature can be studied in detail as an extension to this study. The results of the current work are discussed below.

It was observed from the results that during the month of December, a warm water mass was found to occur every year 30–40 km away from the shoreline, as seen in Fig. 3a. The standard deviation in SST in these areas shows a stable condition during the month for every year of the study period. Due to the consistent nature of this warm water mass, it can be assumed that it is part of an eddy structure forming off the coast during the winter months.

However, the near-coastal waters are not affected by this phenomenon and show a large variation, as seen in Fig. 3b. The graphs in Fig. 4a, b delineate this occurrence very well. Aggregated average SST for the month of December was found to be varying mostly near the coastline within 5-km perpendicular distance as emphasized in Fig. 4a.

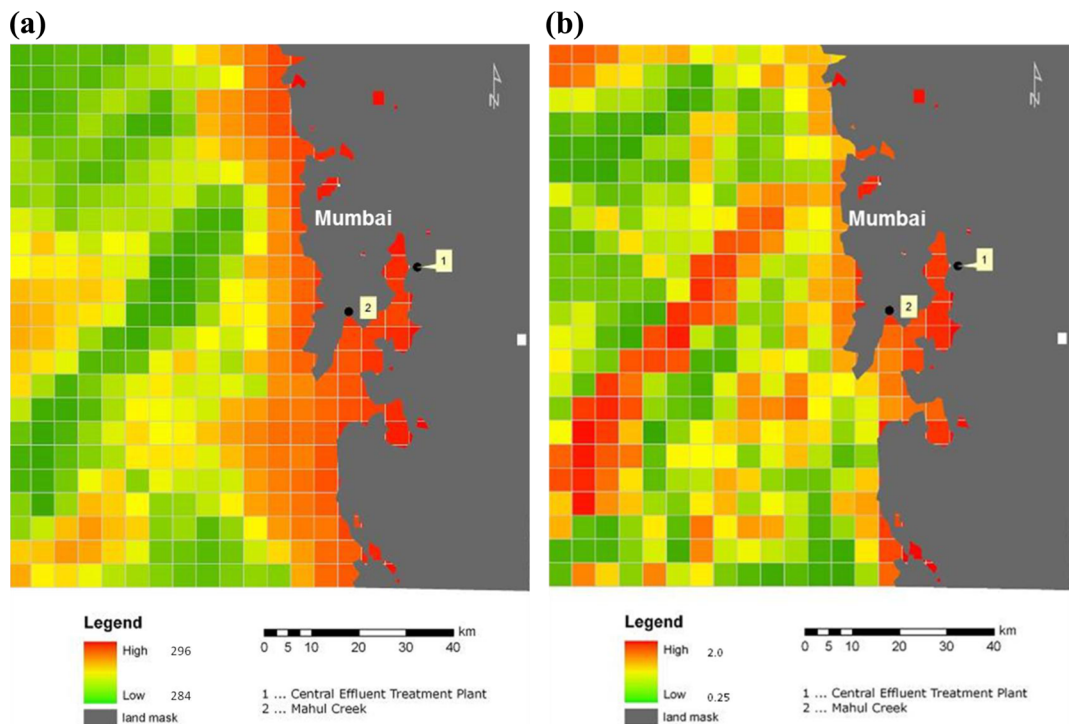**(a)**   **(b)**

Fig. 7 **a** Monthly aggregated average and **b** standard deviation of SST for March (2005–2010)

During the month of January, for most of the years, the warm eddy-like structure just away from the coastline remained in place and intensified (refer to Fig. 5a, b). This warm water structure is corroborated by the findings of Tang et al. (2002, 2005) and Sarangi (2012), who have also reported similar warm water mass in previous works. Because of this meso-scale structure, the coastal waters were perturbed and have shown some random behaviour. However, it can be still seen that the maximum variation is still limited to the first 10-km stretch from the coastline (refer to Fig. 6a, b).

The clumped images reiterate the warm water structure offshore, while showing maximum variability in SST near the coast. Ignoring the possible irregularity and noise in the satellite data, the trends show a temperature disturbance in the area which indicates a possible anthropogenic source of warm water in the area.

During the month of March, the open ocean scenario changed with the onset of summer. As seen from March images, the near-coastal waters were throughout warmer than the pelagic ocean zone (Fig. 7a). The warm water eddy-like structure was found to dissipate during this time as the coastal waters grow warmer. The coastal

zone also shows the maximum variation within the study area (refer Fig. 7b).

In the month of March, the open ocean scenario changed due to the onset of summer. As seen from March images (refer to Fig. 7a, b), the coastal waters are throughout warmer than the pelagic ocean zone. The warm water eddy-like structure was found to dissipate during this time as the coastal waters grow warmer. The coastal zone also shows the maximum variation within the study area (standard deviation in SST, Fig. 8b).

The anthropogenic influence is very prominent in the waters from the graphs and satellite images. However, this might have happened because of the warm water formation which was mentioned earlier. This warm water mass has been forming every year very close to the creek mouth, thus masking the effect of any landward source of heat. However, as this warm water is dissipated, from the colder month of January till the onset of summer in March, all through the study period of 2005–2010, the water of the Vashi creek remained warmer than the waters off a 5-km buffer zone from shoreline. In Figs. 9 and 10, the difference in SST of these two areas has been shown for each year. The average trend given for the area is the aggregated average for all the years.
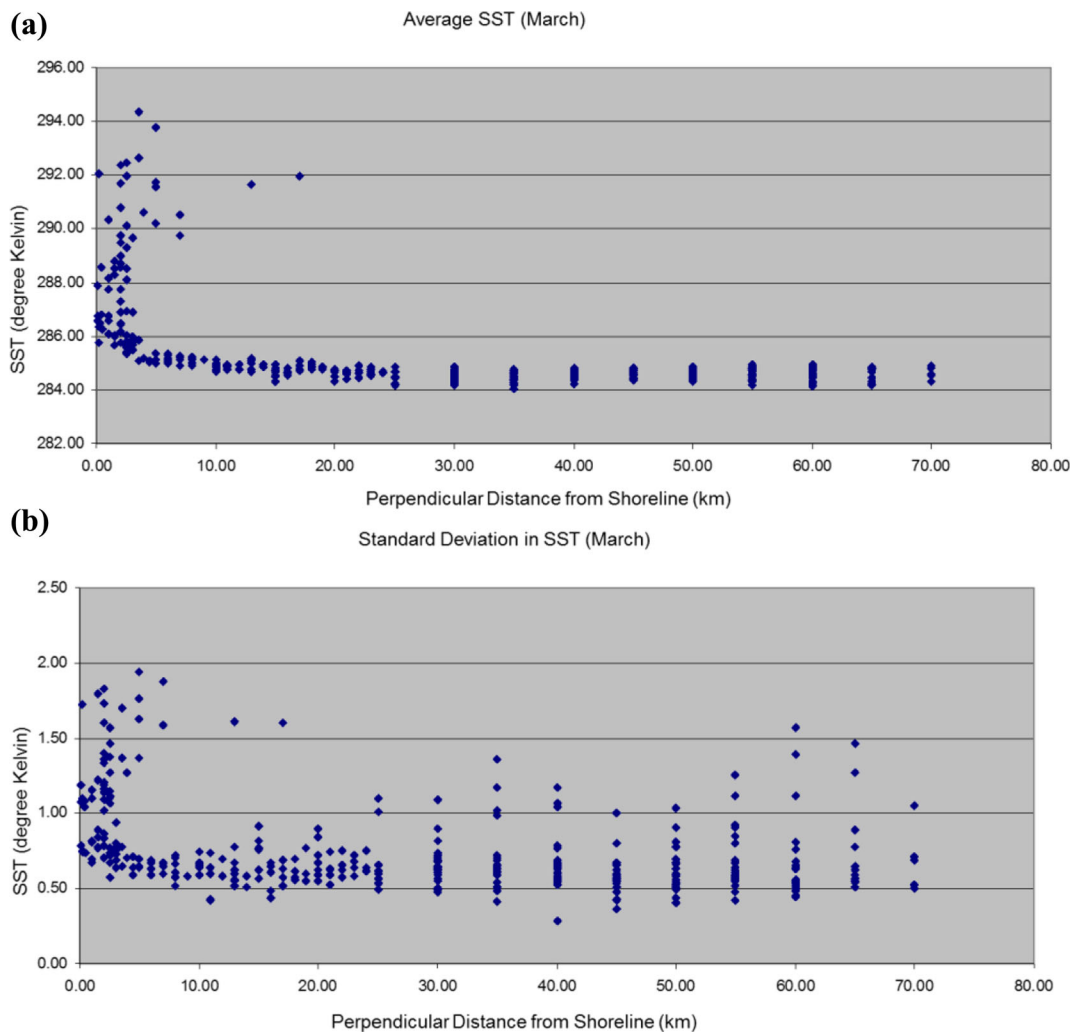
(a)

(b)

Fig. 8 Relationship of **a** average and **b** standard deviation of SST with perpendicular distance from shoreline for March

Similar trends have been generated for the Mahul Creek region shown in Figs. 9 and 10.

Mahul Creek, situated in a bay area which has lesser impact from the change in pelagic water mass, consistently shows higher temperature than the 5-km off the coastline buffer. The surface temperature of these waters is consistently warmer than the offshore areas. Apart from this, a significant drop in overall temperature can be seen in the year 2006 very prominently in this area. This decrease is seen to be increasing from December 2005 to March 2006. Coincidentally, the year 2006 happened to be a La Niña year (Bhuiyan et al. 2006; NOAA 2006). Because of this atmosphere-ocean coupled phenomenon, temperature in the Indian Ocean is known to go down by several degrees, which happens

in a 3–5-year cycle. The effect is seen in the Vashi CETP area also during the month of March, when the climatologic phenomenon was in full sway.

The area near Vikhroli also shows high thermal anomaly with respect to the 5-km buffer specified before. This area is known to harbour a good growth of mangroves, and high temperature in the coastal waters could harm the vulnerable eco-system there. A similar SST anomaly is found throughout the study period near the Ulhas River mouth and several upstream locations.

During the months of January and December, warm water masses are seen to form consistently in the deep sea (~40 km away from land), having higher temperatures in all the years. This may be a part of some mesoscale eddy feature, or warm current offshoot parallel to
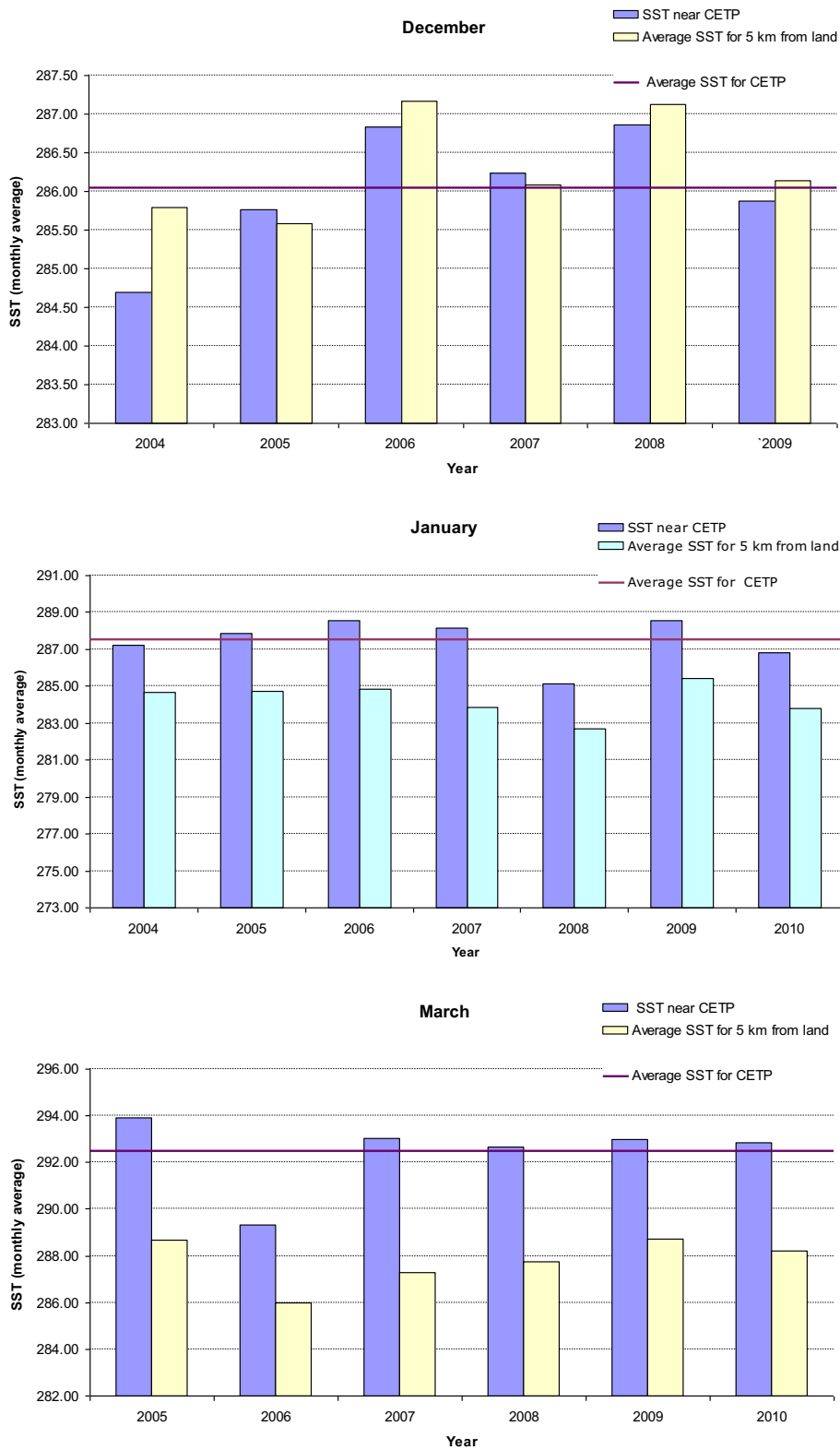
December

January

March

Fig. 9 Comparative SST trend near Vashi (CETP) with respect to the average SST 5 km away from shoreline for the study period. Aggregated average SST in kelvin is shown
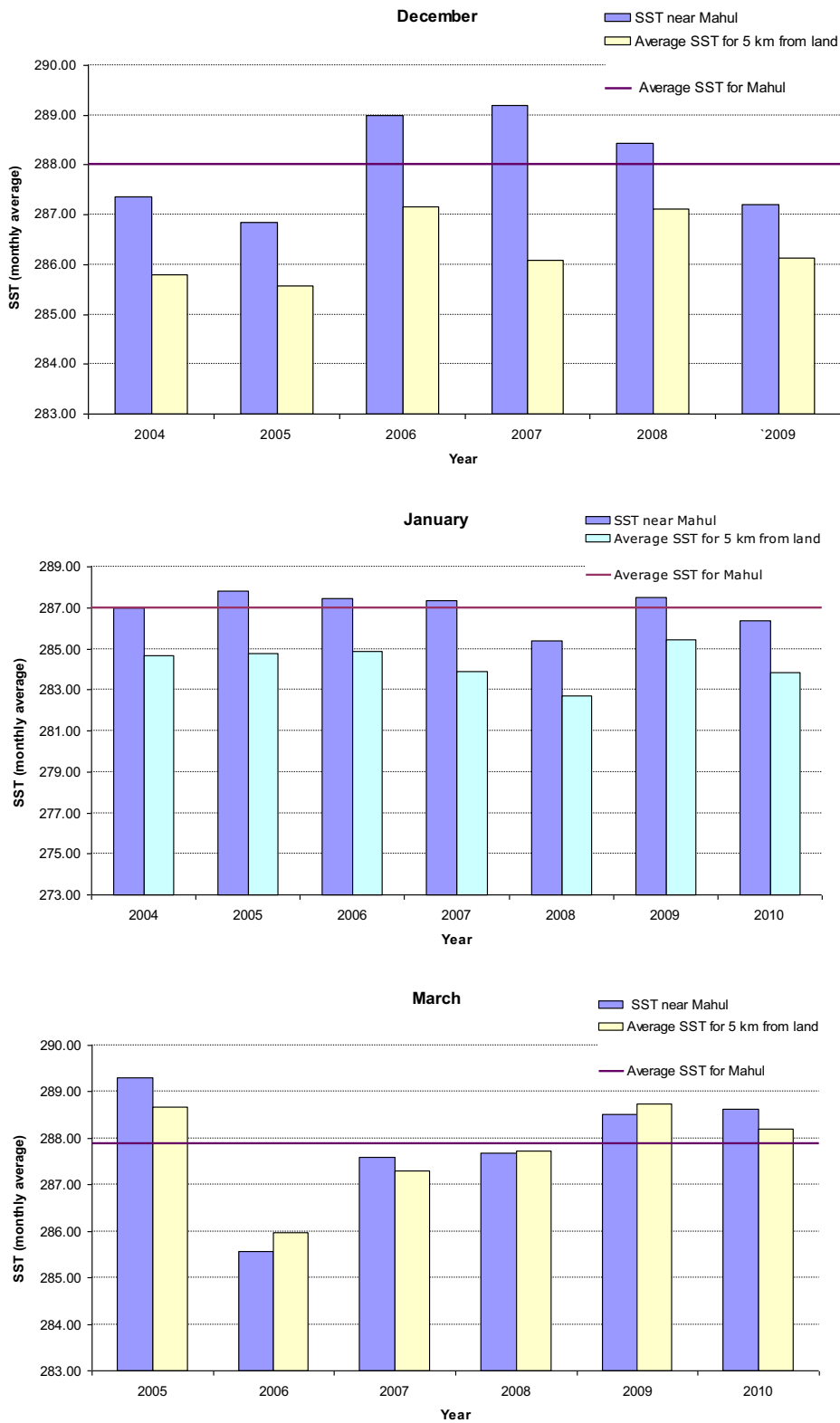
Fig. 10 Comparative SST trend near Mahul Creek area with respect to the average SST 5 km away from shoreline for the study period. Aggregated average SST in kelvin is shown

the shore. This phenomenon could be related to the coastal wintertime upwelling and should be investigated further through thorough temporal studies.

In general, as found from the above standard deviation curves for all 3 months, SST deviations are highest in all the cases nearest to the shoreline. Since anomalies are found in Vashi (CETP) and Mahul Creek areas, SST variation trend has been generated for these two areas. The graphical representation is given in Figs. 9 and 10 respectively.

Summary and conclusions

Due to the global nature of the SST algorithm applied here, the estimated SST in the study area was found to be consistently lower by 7–8 K than the sea-truth measurements. This difference can be attributed to the global algorithms and influence due to local land mass; however, as this error was found to be continuous and consistent, and as the study is qualitative than quantitative, no correction has been applied to the images. It is found that there is a need to modify the available global SST algorithm or generate a local algorithm to cater to the need of this specific area for pre- and post-monsoon seasons. Data during monsoon has been omitted because of the 60–100 % cloud cover during the period of May–October.

Even as qualitative comparison, the observations from the SST images clearly indicate prominent anthropogenic sources of thermal pollution and emphasize the need for remedial action in terms of thermal influx as well as in policies governing release of effluents in the coastal environment.

The variation in SST is found to decrease as the distance increases from shoreline, that is, the highest possible variation in SST is found near the coast. Away from the coastline, the waters are seasonally very stable. For the month of December, the waters near Vashi Creek were found to be less warm than the waters 5 km off the coast. Further, it is found that the overall temperature has been increasing in the coastal waters within the short span of 7 years (2004–2010). Apart from 2006, which was a La Niña year, the SST has increased from the year 2004 to 2010.

To summarize, this study has successfully shown the usefulness of MODIS TIR data in monitoring tropical coastal waters. The effect of temperature change on the various species of organisms is out of scope of the current work. This effect of temperature can be studied in detail as an extension to this study. It was found that a major hurdle faced during this study was the unavailability of historic sea-truth data and collection of sea-truth data from primary and secondary sources that could be used to corroborate the findings from this study. However, the consistent higher temperatures of some of the coastal locations situated close to major sources of effluents are effectively brought out by this study and provide clear directions for further detailed study.

Conflict of interest The authors have declared that no competing interest exists

References

Bhuiyan, C., Singh, R. P., & Kogan, F. N. (2006). Monitoring drought dynamics in the Aravalli region (India) using different indices based on ground and remote sensing data. *International Journal of Applied Earth Observation and Geoinformation, 8*(4), 289–302.

Brown, O.B., Minnett, P.J., Evans, R., Kearns, E., Kilpatrick, K., Kumar, A., Sikorski, R., & Závody, A. (1999). MODIS Infrared Sea Surface Temperature Algorithm, Algorithm Theoretical Basis Document Version 2.0. University of Miami.

Gupta, S. (2005). Climate: Mumbai/Bombay pages. http://theory.tifr.res.in/bombay/physical/climate/. Accessed: June, 2014.

Gupta, I., Dhage, S., Jacob, N., Navada, S., & Kumar, R. (2006). Calibration and Validation of Far Field Dilution Models for Outfall at Worli, Mumbai. *Environmental Monitoring and Assessment, 114*(1), 199–209.

John, J. E. A. (1971). Thermal Pollution: A Potential threat to our aquatic environment. *Environmental Affairs, 1*(2), 287–298.

Kulkarni, V. A., Naidu, V. S., & Jagtap, T. G. (2011). Marine ecological habitat: A case study on projected thermal power plant around Dharamtar creek, India. *Journal of Environmental Biology, 32*(2), 213–219.

Masuoka, E., Tilmes, C., Ye, G., & Devine, N. (2000). Producing global science products for the MODerate resolution Imaging Spectroradiometer (MODIS) in MODAPS. *Geoscience and*

Remote Sensing IEEE International Symposium. doi:10. 1109/igarss.2000.858267.

McClain, C. R. (2009). A Decade of Satellite Ocean Color Observations. *Annual Review of Marine Science, 1*, 19–42.

Meoweather (2013). Mumbai weather history. Mumbai average weather by month. Weather history for Mumbai, Maharashtra, India; http://www.meoweather.com/history/India/na/18.975/72.825833/Mumbai.html?units=c#, Accessed: June, 2013.

Minnett, P. J. (1990). The regional optimization of infrared measurements of sea-surface temperature from space. *Journal of Geophysical Research, 95*, 13,497–13,510. doi:10.1029/JC095iC08p13497.

MPCB. (2010). *Maharashtra Pollution Control Board.* Navi Mumbai: Action plan for Industrial cluster.

NOAA (2006). NOAA News Online (Story 2572), http://www.noaanews.noaa.gov/stories2006/s2572.htm, Accessed: June, 2010.

Sarangi, R. K. (2012). Observation of Oceanic Eddy in the Northeastern Arabian Sea Using Multisensor Remote Sensing Data. *International Journal of Oceanography.* doi: 10.1155/2012/531982.

Tang, D., Kawamura, H. & Luis, A. J. (2002). Short-term variability of phytoplankton blooms associated with a cold eddy in the northwestern Arabian Sea. *Remote Sensing of Environment, 81*(1), 82–89. doi:10.1016/S0034-4257(01)00334-0.

Tang, D., Satyanarayana, B., Singh, R. P. and Zhao, H. (2005). Satellite Remote Sensing of Chlorophyll-a Distribution in the Northeast Arabian Sea. http://www.isprs.org/publications/related/ISRSE/html/papers/954.pdf, Accessed: November, 2010.

Vaquer-Sunyer, R., & Duarte, C. M. (2011). Temperature effects on oxygen thresholds for hypoxia in marine benthic organisms. *Global Change Biology, 17*, 1788–1797.

Varkey, M. J. (1999). Pollution of coastal seas. Indian Academy of Sciences, Bangalore, India, Vol-4, 36-44p.

Verma, A., Balachandran, S., Chaturvedi, N., & Patil, V. (2004). A preliminary report on the biodiversity of Mahul Creek, Mumbai, India with special reference to avifauna. *Zoos' Print Journal, 19*(9), 1599–1605.

Yang, J., Gong, P., Fu, R., Zhang, M., Chen, J., & Liang, S. (2013). The role of satellite remote sensing in climate change studies. [Review]. *Nature Climate Change, 3*(10), 875–883. doi:10.1038/nclimate1908.